Mineral Precipitation from Soda Brines, Lake Magadi, Rift Valley (Kenya)

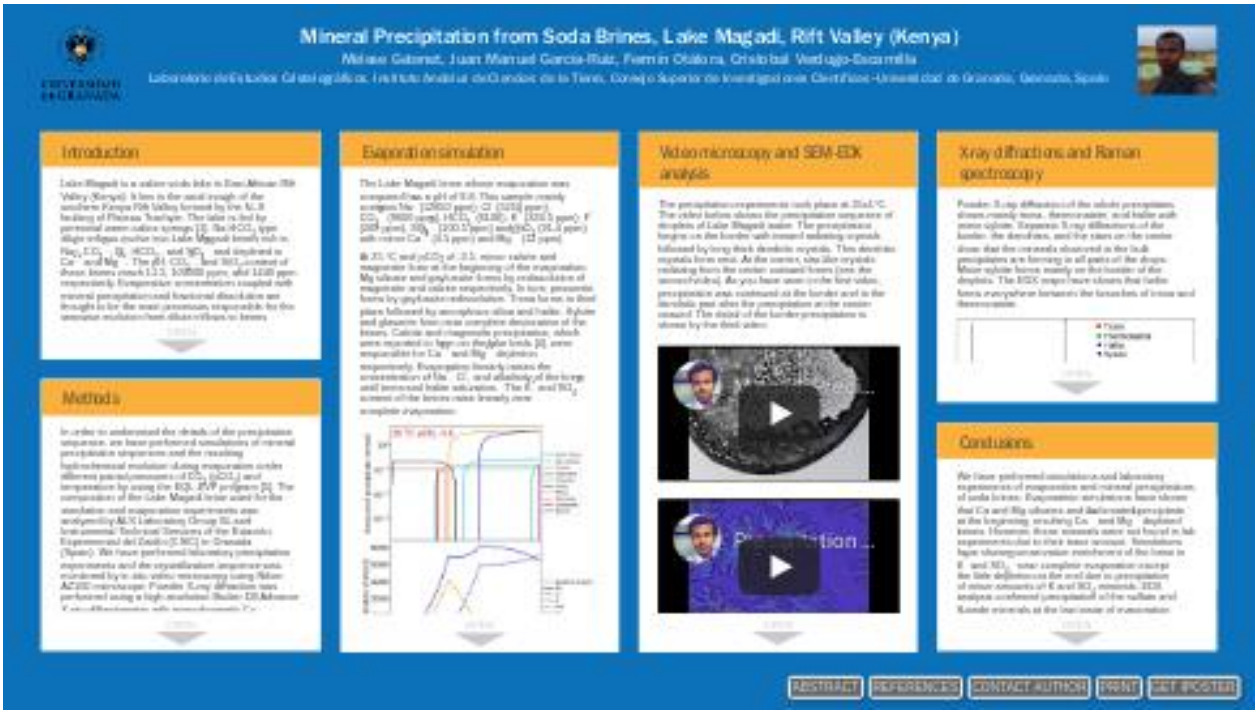

Melese Getenet, Juan Manuel García-Ruiz, Fermín Otálora, Cristobal Verdugo-Escamilla

Laboratorio de Estudios Cristalográficos, Instituto Andaluz de Ciencias de la Tierra (CSIC-UGR), Armilla, Granada, Spain

PRESENTED AT:

INTRODUCTION

Lake Magadi is a saline soda lake in East African Rift Valley (Kenya). It lies in the axial trough of the southern Kenya Rift Valley formed by the N–S faulting of Plateau Trachyte. The lake is fed by perennial warm saline springs [1]. Na-HCO_3 type dilute inflows evolve into Lake Magadi brines rich in Na^+, CO_3^{2-}, Cl^-, HCO_3^-, and SO_4^{2-} and depleted in Ca^{2+} and Mg^{2+}. The pH, CO_3^{2-}, and SiO_2 content of these brines reach 11.5,

109000 ppm, and 1440 ppm respectively. Evaporative concentration coupled with mineral precipitation and fractional dissolution are thought to be the main processes responsible for the stepwise evolution from dilute inflows to brines [2,3]. Ca and Mg carbonate precipitation in rift valley sediments are thought to be the reason for Ca^{2+} and Mg^{2+} depletion [4]. Evaporation and subsequent rise in solute content push Lake Magadi brine until saturation with respect to multiple salts. Here, we present the simulation of evaporation and mineral precipitation and the resulting hydrochemical evolution of the brines as well as laboratory precipitation experiments and characterization of the minerals.

METHODS

In order to understand the details of the precipitation sequence, we have performed simulations of mineral precipitation sequences and the resulting hydrochemical evolution during evaporation under different partial pressures of CO_2 (pCO_2) and temperature by using the EQL-EVP program [5]. The composition of the Lake Magadi brine used for the simulation and evaporation experiments was analyzed by ALS Laboratory Group SL and Instrumental Technical Services of the Estación Experimental del Zaidín (CSIC) in Granada (Spain). We have performed laboratory precipitation experiments and the crystallization sequence was monitored by in situ video microscopy using Nikon AZ100 microscope. Powder X-ray diffraction was performed using a high-resolution Bruker D8 Advance X-ray diffractometer with monochromatic Cu $K_{\alpha 1}$ radiation, primary Ge(111) monochromator, and a Lynxeye PSD detector in our lab. Powder X-ray diffraction was recorded in transmission mode for one hour from 5° to 80° 2θ. Mineral phases were identified using Malvern Panalytical HighScore software (version 4.8) with the ICCD PDF-2 database. Raman spectra were recorded by using a HORIBA Jobin Yvon LabRAM high-resolution Raman spectrometer equipped with an Olympus BX41 optical microscope with binocular and Koehler illumination and a charge-coupled device detector at an excitation wavelength of 532 nm (frequency-doubled neodymium-doped yttrium-aluminium-garnet laser). The texture and chemical composition of the precipitates were studied by using a Zeiss Supra 40VP field-emission scanning electron microscope (SEM) equipped with an Oxford energy-dispersive X-ray analyzer (EDX) at the Centro de Instrumentación Científica (CIC) of the University of Granada (Spain).

EVAPORATION SIMULATION

The Lake Magadi brine whose evaporation was computed has a pH of 9.8. This sample mainly contains Na^+ (12850 ppm), Cl^- (5250 ppm), CO_3^{2-} (9600 ppm), HCO_3^- (6100), K^+ (228.5 ppm), F^- (208 ppm), SO_4^{2-} (100.5 ppm) and SiO_2 (91.4 ppm) with minor Ca^{2+} (4.5 ppm) and Mg^{2+} (12 ppm).

At 25 °C and pCO_2 of -3.5, minor calcite and magnesite form at the beginning of the evaporation. Mg silicate and gaylussite forms by redissolution of magnesite and calcite respectively. In turn, pirssonite forms by gaylussite redissolution. Trona forms in third place followed by amorphous silica and halite. Sylvite and glaserite form near complete desiccation of the brines. Calcite and magnesite precipitation, which were reported to form on the lake beds [4], were responsible for Ca^{2+} and Mg^{2+} depletion respectively. Evaporation linearly raises the concentration of Na^+, Cl^-, and alkalinity of the brine until trona and halite saturation. The K^+ and SO_4^{2-} content of the brines raise linearly near complete evaporation.

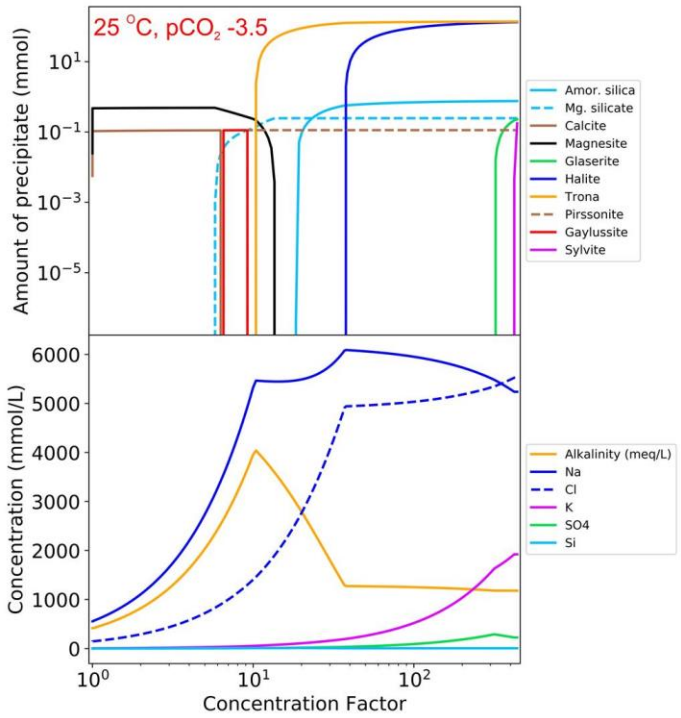

As shown in the next figure, thermonatrite forms instead of trona at high temperature and low pCO_2. Halite forms after thermonatrite. Calcite and magnesite form first followed by Mg silicate, amorphous silica, and pirssonite. Amorphous silica precipitation was delayed significantly due to its high solubility at high temperature. Solute contents raise linearly until mineral precipitation. Coupled precipitation of thermonatrite and halite causes a decline in Cl^-.

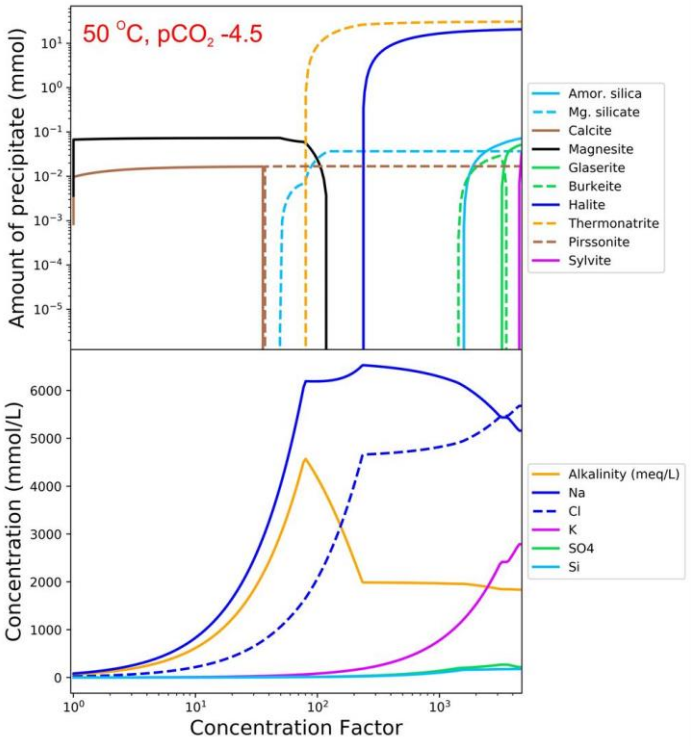

At higher pCO_2 level, nahcolite forms as the major carbonate mineral (see figure below). Nahcolite forms in little Lake Magadi where magmatic CO_2 release through faults has been reported [6-8].

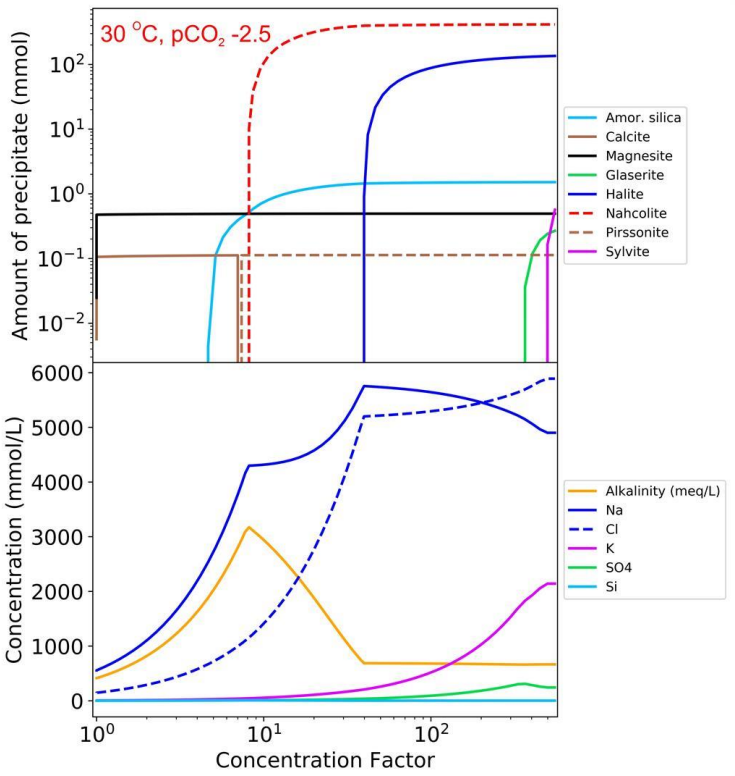

The simulation has shown that Mg and Ca carbonate and silicate minerals form at the beginning causing depletion in Ca^{2+}, Mg^{2+}, and SiO_2. Silica precipitate as siliceous gels in the northern Lake Magadi area. Gaylussite and pirssonite have been reported as the authigenic minerals of Lake Magadi sediments [4]. A minor amount of K^+ and SO_4^{2-} containing minerals (glaserite, burkeite, thenardite, sylvite) form at the very end of the evaporation causing conservative K^+ and SO_4^{2-} enrichment. However, bacterial reduction of sulfate was reported to deplete the SO_4^{2-} level of the lake brines [4]. The major minerals forming during evaporation are trona, thermonatrite, nahcolite, and halite.

VIDEO MICROSCOPY AND SEM-EDX ANALYSIS

The precipitation experiments took place at 25±1°C. The first video (see the the supplemental link https://doi.org/10.6084/m9.figshare.13490346) shows the precipitation sequence of droplets of Lake Magadi water. The precipitation begins on the border with inward radiating crystals followed by long thick dendritic crystals. Thin dendritic crystals form next. At the center, star-like crystals radiating from the center outward forms (see the supplemental link https://doi.org/10.6084/m9.figshare.13490346). As you have seen in the first video, precipitation was continued at the border and in the dendritic part after the precipitation at the center ceased. The detail of the border precipitation is shown by the third video (see the supplemental link https://doi.org/10.6084/m9.figshare.13490346).

The figure below shows the EDX map of the precipitates forming at the border, the dendrites, and the star-shaped precipitates at the center. The precipitates are mainly Na-CO_3 minerals (trona and

thermonatrite) with halite on top of the Na-CO_3 minerals on the border and between the branches of the dendrites and star-shaped crystals. Halite forms after the dendrites and the star-shaped crystals. On the border, minor fluorine and sulfur were detected with EDX, implying the minor amount of villiaumite and sulfate minerals that form at the end of the evaporation simulation. Ca, Mg, K, and Si were not detected with EDX because of their trace amount (see the simulations).

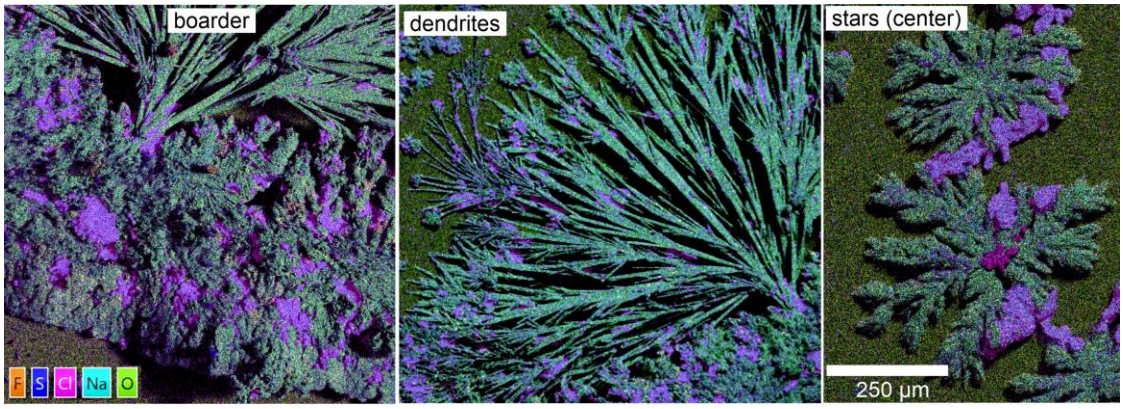

X-RAY DIFFRACTIONS AND RAMAN SPECTROSCOPY

Powder X-ray diffraction of the whole precipitates shows mainly trona, thermonatrite, and halite with minor sylvite. Separate X-ray diffractions of the border, the dendrites, and the stars on the center show that the minerals observed in the bulk precipitates are forming in all parts of the drops. Minor sylvite forms mainly on the border of the droplets. The EDX maps have shown that halite forms everywhere between the branches of trona and thermonatrite.

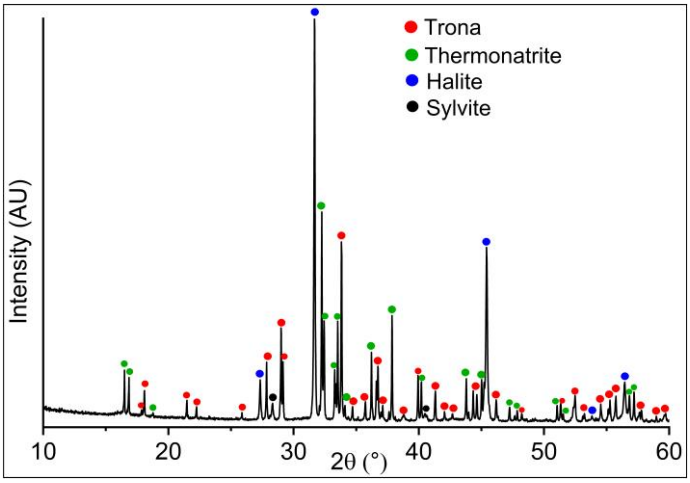

As shown below, Raman spectra of the border revealed trona (green dots) and thermonatrite (red dots) at the bottom of the trona crust. The trona and thermonatrite represent the first dendritic minerals on the border and the minerals forming at the end (after drying of the center of the drop) as shown in the first and third videos respectively. As observed in EDX maps, the trona forming at the beginning was covered by halite.

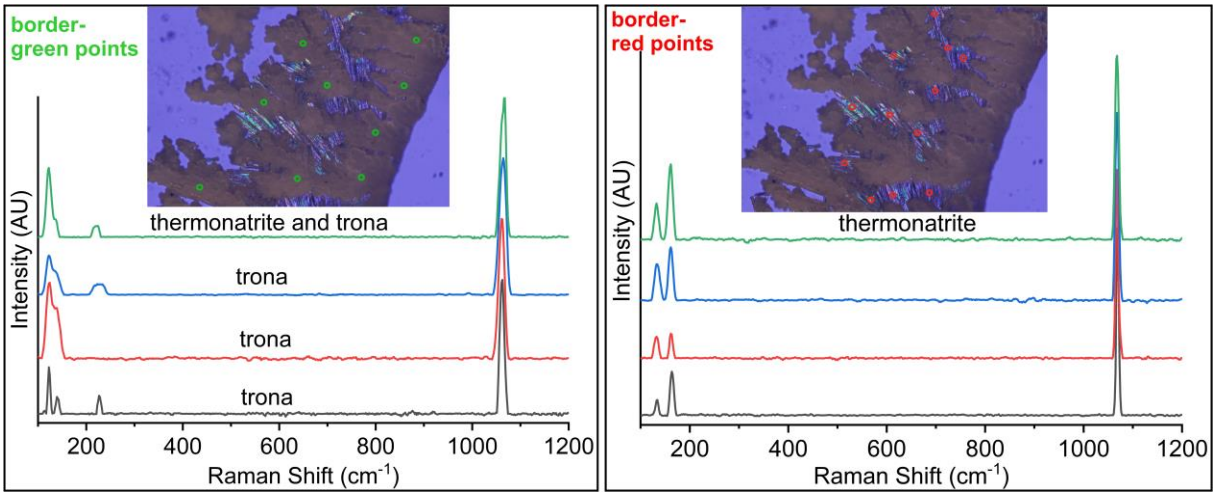

As shown below, the thick (green rectangle) and thin (red rectangle) dendrites that precipitate following the border precipitation were trona. Halite forms between these branches (see EDX map of dendrites).

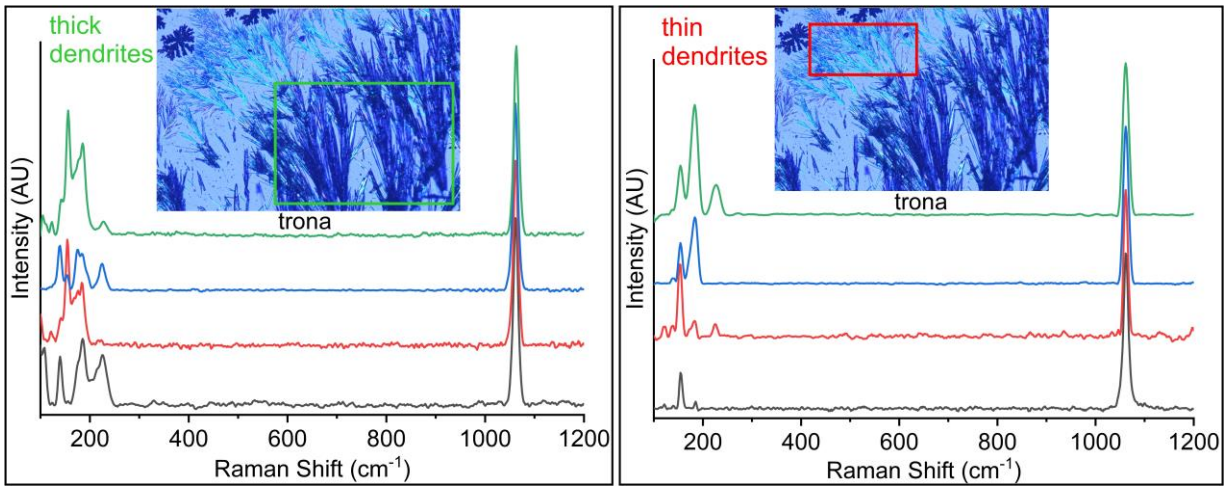

At the center of the drop, the outward radiating star-shaped minerals were mainly thermonatrite with trona (see figure below). As shown by the second video, the precipitation at the center resembles that of the border implying trona precipitation followed by thermonatrite and finally halite. The EDX analysis of the stars (on the center) and dendrites has shown that halite forms after trona and thermonatrite in between the radiating branches. After desiccation of the center of the drop, thermonatrite form at the bottom of the trona and halite crust at the border (see red points on the border). At the local scale (at the center and at the branches), halite seems to form last but thermonatrite forms at the border after the desiccation of the center of the drops. The video microscopy, Raman spectra, and EDX analysis show that the precipitation begins with trona followed by halite and finally thermonatrite.

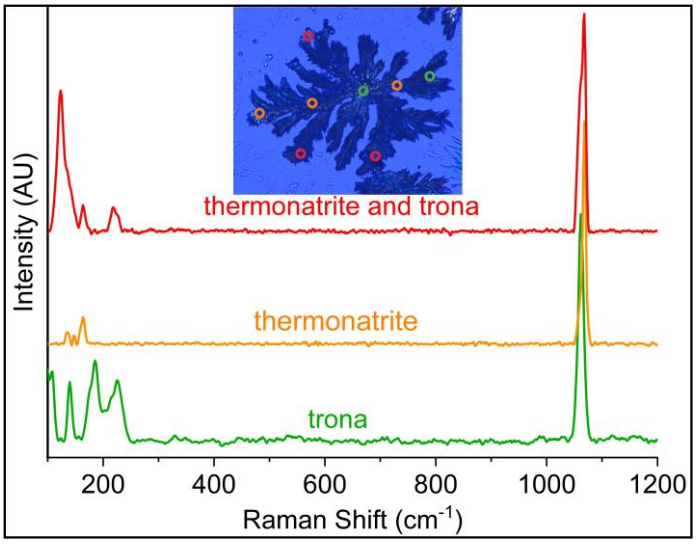

CONCLUSIONS

We have performed simulations and laboratory experiments of evaporation and mineral precipitations of soda brines. Evaporation simulations have shown that Ca and Mg silicates and carbonates precipitate at the beginning, resulting Ca^{2+} and Mg^{2+} depleted brines. However, these minerals were not found in lab experiments due to their trace amount. Simulations have shown conservative enrichment of the brine in K^+ and SO_4^{2-} near complete evaporation except the little depletion at the end due to precipitation of minor amounts of K and SO_4 minerals. EDX analysis confirmed precipitation of the sulfate and fluoride minerals at the last stage of evaporation covering trona and thermonatrite. Evaporation enriches Na^+, Cl^-, and alkalinity of the brines linearly until saturation in trona, thermonatrite, nahcolite, and halite. The precipitation of these phases depletes the Na^+, Cl^-, and alkalinity of the brines. X-ray diffraction and Raman spectroscopy have shown thermonatrite precipitation after trona following the depletion of the brines in HCO_3^- during trona precipitation. Nahcolite precipitation was observed only in simulations and its absence in lab experiments could be due to the lack of CO_2 supply and the dominance of the chemistry of the water by CO_3^{2-} ions over HCO_3^-. The simulations and evaporation experiments have shown that the precipitation sequence of the major minerals was trona, halite, and thermonatrite. This sequence of precipitation has been confirmed by in situ synchrotron X-ray diffraction of the minerals forming during evaporation of acoustically levitated droplets of Lake Magadi brine. The combination of modeling and in situ mineralogical analysis is a powerful tool to understand mineral assemblages, kinetic precipitation pathways, and the resulting hydrochemical evolution of soda lakes.

REFERENCES

[1] Baker, B.H. Geology of the Area south of Magadi; Geological Survey of Kenya: Nairobi, Kenya, 1963; Volume 61, p. 27.

[2] Eugster, H.P. Chemistry and origin of the brines of Lake Magadi, Kenya. Miner. Soc. Amer. Spec. Pap. 1970, 3, 213–235.

[3] Jones, B.F.; Eugster, H.P.; Rettig, S.L. Hydrochemistry of the Lake Magadi basin, Kenya. Geochim. Cosmochim. Acta 1977, 41, 53–72.

[4] Eugster, H.P. Lake Magadi, Kenya, and Its Precursors. In Developments in Sedimentology; Nissenbaum, A., Ed.; Elsevier: Amsterdam, The Netherlands, 1980; Volume 28, pp. 195–232.

[5] Risacher, F.; Clement A. A computer program for the simulation of evaporation of natural waters to high concentration Comput. Geosci., 27 (2001), pp. 191-201.

[6] Lee, H.; Muirhead, J.D.; Fischer, T.P.; Ebinger, C.J.; Kattenhorn, S.A.; Sharp, Z.D.; Kianji, G. Massive and prolonged deep carbon emissions associated with continental rifting. Nat. Geosci. 2016, 9, 145–149.

[7] Lowenstein, T.K.; Demicco, R.V. Elevated Eocene Atmospheric CO2 and Its Subsequent Decline. Science 2006, 313, 1928.

[8] Renaut, R.W.; Owen, R.B.; Lowenstein, T.K.; De Cort, G.; Mcnulty, E.; Scott, J.J.; Mbuthia, A. The role of hydrothermal fluids in sedimentation in saline alkaline lakes: Evidence from Nasikie Engida, Kenya Rift Valley. Sedimentology. 2020.